ikenga International
journal of institute of african studies
Vol. 25, No 1, January 2024

ISSN: 2006-4241
E-ISSN : 2714-4321

Exploring the Role of Vaccination in Achieving Herd Immunity for Covid-19: A SEIQRD Model Study

Widowati*[1], Tiara Nurdianti [2], Eka Triyana[3], Taleb Gaber[4]

[1,2,3,4]Department of Mathematics, Faculty of Sciences and Mathematics, Diponegoro University, Semarang, 50275, Indonesia

***Corresponding author:** widowati@lecturer.undip.ac.id

Abstract

The Covid-19 pandemic poses a serious global health risk as an infectious disease transmitted from human to human. Starting In the early months of 2021, vaccination drives were launched to trigger collective defences through population immunity and lower rates of infections. This study examined a SEIQRD model adding vaccination to analyse the spread of COVID-19. Two equilibrium states exist: non-endemic and endemic. Local stability near the equilibria was determined using Routh-Hurwitz criteria. Global stability was assessed through Lyapunov analysis of overall disease dynamics. Stability relies on the basic reproduction number ($\mathfrak{R}_0$) *from Next Generation Matrix calculations. Stability analysis showed the system asymptotically stable with a bifurcation at* $\mathfrak{R}_0 = 1$. *Numerical solutions via fifth-order Runge-Kutta integration simulated in MATLAB found* $\mathfrak{R}_0 = 0.0004032$, *indicating local and global asymptotic stability. The study findings indicate that infections inevitably diminish over the long run. Sensitivity analysis identified four critically influential factors: the pace of introducing susceptible into the population, the likelihood of contracting the virus, the speed of developing symptoms after exposure, and the natural rate of mortality. Small variations in any of these four parameters can significantly impact projected disease dynamics. Close examination of their effects provides guidance on intervention strategies likely to shape the outbreak's trajectory. Finally, a forward bifurcation driven by the value of* $\mathfrak{R}_0$ *was detected.*

Keywords: *Covid-19, Runge-Kutta, Lyapunov, Routh-Hurwitz, SEIQRD, Forward, Bifurcation*

Introduction

In early 2020, the international community was alarmed by reports of unknown, severe Pneumonia originating in Wuhan, China. Chinese authorities first notified the World Health Organization (WHO) of 44 such cases among residents on December 31st, 2019 (Levani et al., 2021; Mukherjee et al., 2023; Peter et al., 2021). Coronaviruses comprise a significant family of viruses capable of infecting both humans and other animals. When transmitted to people, they can manifest as respiratory illnesses ranging from mild conditions like the common cold to more serious diseases such as Middle East Respiratory Syndrome (MERS) and Severe Acute Respiratory Syndrome (SARS) (Khan et al., 2021; Sherif et al., 2023; Legesse et al., 2023). Thus, this particular illness was designated Coronavirus Disease-2019 (COVID-19) (Nasution et al., 2021; Han et al., 2020; Wu et al., 2020).

The lungs represent the organs most prominently impacted by COVID-19, as the virus preferentially engages host cells via the ACE2 receptor protein abundantly situated in type II alveolar cells within the lungs (Letko et al., 2020; Sinaga et al., 2021). Airborne dissemination allows the coronavirus to persist suspended for up to three hours, and surfaces provide alternate routes for indirect transmission over prolonged durations. Diagnostic categorization of COVID-19 involves suspected, probable and confirmed case classifications (Fatima et al., 2020; Yang & Wang, 2020; Schecter, 2021). Mass vaccination emerged as a core strategy adopted by governments to ultimately overcome the pandemic (Kolawole et al., 2023; Sahu & Singh, 2023; Savina et al., 2022) resembling earlier initiatives that halted plagues like polio and smallpox before definitive treatments emerged.

Mathematical modelling constitutes a principal analytical approach applied to epidemic preparedness, including addressing the COVID-19 crisis (Shah & Mittal, 2021; Hamed, 2022; Shah & Chaudhary, 2023). Such modelling facilitates comprehending, simplifying and solving real-world problems through numerical methods serving as an alternative to closed-form analytical solutions obtainable via standard algebraic formulas (Hossain, 2017; Owolabi et al., 2019; Parsamanesh et al., 2019; Annas et al., 2020; Kamrujjaman et al., 2022). Prior research by Chapra and Canale (2015) found the fifth-order Runge-Kutta technique exhibited less error than lower-order versions, confirming its enhanced accuracy.

This study analysed the framework proposed by Mamo (2020), extending it by incorporating vaccination into susceptible subgroups while excluding the "H" or home isolation category. The resultant SEIQRD model partitions the population into six classes: susceptible

(S), latently exposed (E), symptomatic infections (I), isolated/quarantined cases (Q), recovered/immune (R), and deaths (D).

Construction Of Model

This research relies upon several key assumptions. It considers the overall population sufficiently large and open, allowing for natural increases and decreases through birth and death. The baseline mortality rate (μ) is assumed uniform across subpopulations. Initial conditions and parameter values must be non-negative numbers. Successfully vaccinated susceptible individuals transition to the recovered class.

Figure 1: Schematic of the spread of COVID-19

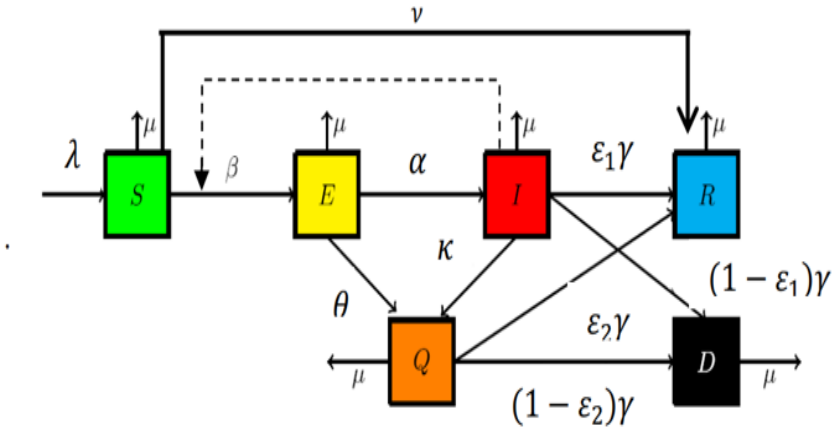

Susceptible (S) individuals represent the currently healthy but vulnerable segment. S numbers rise through new recruitment at rate λ but fall as contacts with infecteds (I) expose some to the virus at rate βI. Vaccination (v) and natural death (μ) also decrement S. The exposed or latent group (E) comprises those exposed but not yet symptomatic, during incubation which averages 14 days. E rises from new exposures at rate βI then falls as some develop symptoms at rate α or isolate prematurely at rate θ. Natural death also decreases E. Infected (I) covers those symptomatic. I increases from the incubating group at rate α, then decreases as some isolate at rate κ or recover/die at rate γ, in addition to natural mortality. Quarantined (Q) captures isolated clinical cases. Q receives input from incubating (θ) and symptomatic (κ) individuals. Output flows to recovery ($\gamma\varepsilon_2$) or death $\big(\gamma(1-\varepsilon_2)\big)$, along with the background mortality rate. Recovered/immune individuals (R) increase through vaccination (v), recovery from symptoms ($\gamma\varepsilon_1$), or post-isolation ($\gamma\varepsilon_2$). Only natural death depletes R.

Finally, deaths (D) accrue from non-recovery among infected $\left(\gamma(1-\varepsilon_1)\right)$ and quarantines $\left(\gamma(1-\varepsilon_2)\right)$, again experiencing the baseline mortality rate.

Figure 1 schematizes these compartmental flows among the SEIQRD subclasses. The paper models this process using numerical integration via the Runge-Kutta method. Thus obtained a mathematical model of the spread of Covid-19 which consists of six differential equations as follows.

$$\begin{cases} \frac{dS}{dt} = \lambda - \beta SI - (\nu + \mu)S \\ \frac{dE}{dt} = \beta SI - (\alpha + \theta + \mu)E \\ \frac{dI}{dt} = \alpha E - (\gamma + \kappa + \mu)I \\ \frac{dQ}{dt} = \theta E + \kappa I - (\gamma + \mu)Q \\ \frac{dR}{dt} = \varepsilon_1 \gamma I + \varepsilon_2 \gamma Q + \nu S - \mu R \\ \frac{dD}{dt} = (1-\varepsilon_1)\gamma I + (1-\varepsilon_2)\gamma Q - \mu D \end{cases} \quad (1)$$

Basic Reproduction Number

The basic reproduction number is a parameter used to find out how the rate of spread of Covid-19 virus infection in the population is. To obtain the value of $\mathfrak{R}_0$, the author will use the next generation matrix (NGM) method. Then by using Maple's tools it is obtained:

$$\mathfrak{R}_0 = \frac{\alpha\beta\lambda}{(\alpha + \theta + \mu)(\nu + \mu)(\gamma + \kappa + \mu)}$$

Equilibrium Point

The equilibrium point is a state that explains the change in the number of individuals with time, so the change in the number of individuals with time is zero. Therefore, in the model system of equations (1) it can be written:

$$\lambda - \beta SI - (\nu + \mu)S = 0 \quad (2)$$

$$\beta SI - (\alpha + \theta + \mu)E = 0 \quad (3)$$

$$\alpha E - (\gamma + \kappa + \mu)I = 0 \quad (4)$$

$$\theta E + \kappa I - (\gamma + \mu)Q = 0 \quad (5)$$

The non-endemic equilibrium point is a situation when there is no spread of the Covid-19 virus, so that no more individuals are infected by the Covid-19 virus. Therefore, the subpopulation in the model consisting of individuals indicated to be infected or confirmed

positive for the Covid-19 virus is zero ($E = I = Q = 0$). Then substitute $E = I = Q = 0$ in equation (2) - (5) to get:

$$\mathbb{E}^0 = (S^0, E^0, I^0, Q^0) = \left(\frac{\lambda}{(\nu + \mu)}, 0,0,0\right)$$

The endemic equilibrium point is a condition when the spread of Covid-19 occurs, so that individuals who are indicated to be infected or confirmed positive can transmit the infection to other individuals. In this case it means that $E \neq I \neq Q \neq 0$ as well as R and D are ignored according to the assumption given that individuals recovering from Covid-19 (subpopulation R) will no longer be sick. then obtained the endemic equilibrium point $\mathbb{E}^* = (S^*, E^*, I^*, Q^*)$ with their respective values as follows:

$$S^* = \frac{\lambda}{\beta I^* + (\nu + \mu)}$$

$$E^* = \frac{(\gamma + \kappa + \mu)I^*}{\alpha}$$

$$I^* = \frac{\alpha\beta\lambda - (\alpha + \theta + \mu)(\gamma + \kappa + \mu)(\mu + \nu)}{\beta(\alpha + \theta + \mu)(\gamma + \kappa + \mu)} = \frac{(\Re_0 - 1)(\mu + \nu)}{\beta}$$

$$Q^* = \frac{(\theta\gamma + \theta\kappa + \theta\mu)I^* + \alpha\kappa}{\alpha(\gamma + \mu)}$$

Stability Analysis of the Equilibrium Point

Stability analysis can be used to determine the behaviour around the equilibrium point. Stability analysis is carried out at the non-endemic equilibrium point and the endemic equilibrium point which will then be proven by the following theorems:

Theorem 1. *If* $\Re_0 < 1$, *the non-endemic equilibrium* $\mathbb{E}^0$ *will be locally asymptotically stable.*

Proof: From the linearization process to determine the Jacobi matrix around $\mathbb{E}^0$, the following matrix is obtained:

$$J(\mathbb{E}^0) = \begin{bmatrix} -\nu - \mu & 0 & -\frac{\beta\lambda}{\nu + \mu} & 0 \\ 0 & -\alpha - \theta - \mu & \frac{\beta\lambda}{\nu + \mu} & 0 \\ 0 & \alpha & -\gamma - \kappa - \mu & 0 \\ 0 & \theta & \kappa & -\gamma - \mu \end{bmatrix}$$

With the Sarrus method and the Maple computing tools, the characteristic equation of Jacobian $J(\mathbb{E}^0)$ is obtained as follows:

$$(x+\nu+\mu)(x+\gamma+\mu)(x^2+(\gamma+\kappa+\alpha+\theta+2\mu)x-\frac{\alpha\beta\gamma}{\mu+\nu}+(\alpha+\theta+\mu)(\kappa+\gamma+\mu))=$$

0 (6)

From equation (6) we obtain eigenvalue are $x_1=-(\gamma+\mu)$, $x_2=-(\nu+\mu)$ and the polynomial equation is $(x+\nu+\mu)(x+\gamma+\mu)(A_0x^2+A_1x+A_2)$, where:

$A_0=1$

$A_1=(\gamma+\kappa+\alpha+\theta+2\mu)$

$A_2=-\frac{\alpha\beta\gamma}{\mu+\nu}+(\alpha+\theta+\mu)(\kappa+\gamma+\mu)=(1-\Re_0)(\alpha+\theta+\mu)(\kappa+\gamma+\mu)$

Based on Routh-Hurwitz criteria, $\mathbb{E}^0$ locally asymptotically stable if $A_1>0$ and $A_1.A_2>0$, these conditions are met if $\Re_0<1$. ■

Theorem 2. *If* $\Re_0>1$, *the endemic equilibrium* $\mathbb{E}^*$ *will be locally asymptotically stable.*

Proof: From the linearization process to determine the Jacobian matrix around $\mathbb{E}^*$, the following matrix is obtained:

$J(\mathbb{E}^*)$

$$=\begin{bmatrix}\frac{-\alpha\beta\lambda+(\alpha+\theta+\mu)(\gamma+\kappa+\mu)(\mu+\nu)}{\beta(\alpha+\theta+\mu)(\gamma+\kappa+\mu)}-\mu-\nu & 0 & -\frac{(\alpha+\theta+\mu)(\gamma+\kappa+\mu)}{\alpha} & 0\\ \frac{\alpha\beta\lambda-(\alpha+\theta+\mu)(\gamma+\kappa+\mu)(\mu+\nu)}{\beta(\alpha+\theta+\mu)(\gamma+\kappa+\mu)} & -\alpha-\theta-\mu & \frac{(\alpha+\theta+\mu)(\gamma+\kappa+\mu)}{\alpha} & 0\\ 0 & \alpha & -\gamma-\kappa-\mu & 0\\ 0 & \theta & \kappa & -\gamma-\mu\end{bmatrix}$$

With the Sarrus method and the Maple computing tools, the characteristic equation of Jacobian $J(\mathbb{E}^*)$ is obtained as follows:

$$(x+\gamma+\mu)(x^3+\left(\frac{((\gamma+\kappa+\mu)\alpha^2+(\lambda\beta+(\gamma+\kappa+\mu)(\gamma+\kappa+2\theta+3\mu))\alpha+(\theta+\mu)(\gamma+\kappa+\mu)(\gamma+\kappa+2\mu+\theta)}{(\gamma+\kappa+\mu)(\theta+\alpha+\mu)}\right)x^2+$$

$$\left(\frac{\lambda\beta\alpha^2+\lambda(\gamma+\kappa+2\mu+\theta)\beta\alpha}{(\gamma+\kappa+\mu)(\theta+\alpha+\mu)}\right)x-\left(\lambda\beta\alpha-(\nu+\mu)(\alpha+\theta+\mu)(\gamma+\kappa+\mu)\right))=0 \qquad (7)$$

From equation (7) we obtain eigenvalue are $x_1=-(\gamma+\mu)$ and the polynomial equation is $(x+\gamma+\mu)(a_0x^3+a_1x^2+a_2x+a_3)$, where:

$a_0=1$

$a_1=\frac{((\gamma+\kappa+\mu)\alpha^2+(\lambda\beta+(\gamma+\kappa+\mu)(\gamma+\kappa+2\theta+3\mu))\alpha+(\theta+\mu)(\gamma+\kappa+\mu)(\gamma+\kappa+2\mu+\theta)}{(\gamma+\kappa+\mu)(\theta+\alpha+\mu)}$

$a_2=\left(\frac{\lambda\beta\alpha^2+\lambda(\gamma+\kappa+2\mu+\theta)\beta\alpha}{(\gamma+\kappa+\mu)(\theta+\alpha+\mu)}\right)$

$a_3=\left(\lambda\beta\alpha-(\nu+\mu)(\alpha+\theta+\mu)(\gamma+\kappa+\mu)\right)$

$a_3 = (\Re_0 - 1)(\nu + \mu)(\alpha + \theta + \mu)(\gamma + \kappa + \mu)$

Based on Routh-Hurwitz criteria, $\mathbb{E}^*$ locally asymptotically stable if $a_1 > 0$, $a_2 > 0$ and $a_1 . a_2 > a_3$, these conditions are met if $\Re_0 > 1$. ■

Theorem 3. *The non-endemic equilibrium points* $\mathbb{E}^0$ *in the model will be globally asymptotically stable if* $\Re_0 < 1$.

Proof: We define the function $V: P \to \mathbb{R}$ with $P = \{(S, E, I, Q, R, D) | S, E, I, Q, R, D \in \mathbb{R}\}$ and the Lyapunov function for the reduced system of equations (1) that is:

$$V(t) = \left(S - S^0 - S^0 ln \frac{S}{S^0}\right) + k_1 E + k_2 I + k_3 Q$$

This Lyapunov function which was used by many authors before see (Saeed, 2017; Gaber et al., 2024). Function V is a Lyapunov function because it fulfils the following conditions: The function V consists of a logarithmic function, so it is clear that the function is a continuous function on P, and the first partial derivative is also a continuous function on P.

The function V has a global minimum at $\mathbb{E}^0$ with respect to all points in P.

For $V(S, E, I, Q) \neq V(S^0, E^0, I^0, Q^0)$ will be shown that $V(S, E, I, Q) > 0$.

$$V = \left(S - S^0 - S^0 ln \frac{S}{S^0}\right) + k_1 E + k_2 I + k_3 Q$$

$$= S^0 \left(\frac{S}{S^0} - 1 - ln \frac{S}{S^0}\right) + k_1 E + k_2 I + k_3 Q$$

It can be seen that the function V will be positive if $S^0 \left(\frac{S}{S^0} - 1 - ln \frac{S}{S^0}\right) > 0$.

Next, we will obtain the Hessian matrix in S^0 and use it to show that S^0 is the global minimum point:

$$H(S^0) = \left[\frac{\partial^2 V}{\partial S^2}\right] = \left[\frac{1}{S^0}\right]$$

Matrix $H(S^0)$ positive definite because $\det\left(H(S^0)\right) = \frac{1}{S^0} > 0$.

For $V(S, E, I, Q) = V(S^0, E^0, I^0, Q^0)$ will be shown that $V(S, E, I, Q) = 0$.

$$V = \left(S - S^0 - S^0 ln \frac{S}{S^0}\right) + k_1 E + k_2 I + k_3 Q$$

$$= \left(\frac{\lambda}{(\nu + \mu)} - \frac{\lambda}{(\nu + \mu)} - \frac{\lambda}{(\nu + \mu)} ln 1\right) + 0 + 0 + 0$$

$$= 0$$

Then it is proved that $V(S,E,I,Q) > 0$ when $V(S,E,I,Q) \neq V(S^0,E^0,I^0,Q^0)$ with $V(S,E,I,Q) \in P$, and $V(S,E,I,Q) = 0$ when $V(S,E,I,Q) = V(S^0,E^0,I^0,Q^0)$, and S^0 is the global minimum.

The derivative of the function V(t) is $\frac{dV(t)}{dt}$ satisfies $\frac{dV(t)}{dt} \leq 0$ for all points in P.

$$\frac{dV}{dt} = \frac{\partial V}{\partial S}\frac{dS}{dt} + \frac{\partial V}{\partial E}\frac{dE}{dt} + \frac{\partial V}{\partial I}\frac{dI}{dt} + \frac{\partial V}{\partial Q}\frac{dQ}{dt}$$

$$= \left(1 - \frac{S^0}{S}\right)\frac{dS}{dt} + k_1\frac{dE}{dt} + k_2\frac{dI}{dt} + k_3\frac{dQ}{dt}$$

$$= \left(1 - \frac{S^0}{S}\right)(\lambda - \beta SI - (\nu+\mu)S) + k_1(\beta SI - (\alpha+\theta+\mu)E) + k_2(\alpha E - (\gamma+\kappa+\mu)I) + k_3(\theta E + \kappa I - (\gamma+\mu)Q)$$

$$= (-k_1(\alpha+\theta+\mu) + k_2\alpha + k_3\theta)E + \left(k_1\beta\left(\frac{\lambda}{(\nu+\mu)}\right) - k_2(\gamma+\kappa+\mu) + k_3\kappa\right)I - k_3(\gamma+\mu)Q$$

$$= \left(-(\alpha+\theta+\mu) + \frac{\alpha\beta\lambda}{(\nu+\mu)(\gamma+\kappa+\mu)}\right)E + \left(\frac{\beta\lambda}{(\nu+\mu)} - \frac{\beta\lambda}{(\nu+\mu)}\right)I$$

$$= \left(\frac{\alpha\beta\lambda}{(\nu+\mu)(\gamma+\kappa+\mu)} - (\alpha+\theta+\mu)\right)E$$

$$= (\Re_0 - 1)(\alpha+\theta+\mu)E$$

When $\Re_0 < 1$, then value $\frac{dV(t)}{dt} \leq 0$. So, it can be concluded that the non-endemic equilibrium points E^0 for the system of equations (1) is globally asymptotically stable. ■

Theorem 4. *The endemic equilibrium points* $\mathbb{E}^*$ *in the model will be globally asymptotically stable if* $\Re_0 > 1$.

Proof: We define the function $W: P \to \mathbb{R}$ with $P = \{(S,E,I,Q,R,D) | S,E,I,Q,R,D \in \mathbb{R}\}$ and the Lyapunov function for the reduced system of equations (1) that is:

$$W(t) = \left(S - S^* - S^* ln\frac{S}{S^*}\right) + \left(E - E^* - E^* ln\frac{E}{E^*}\right) + \left(I - I^* - I^* ln\frac{I}{I^*}\right) + \left(Q - Q^* - Q^* ln\frac{Q}{Q^*}\right)$$

Function W is a Lyapunov function because it fulfils the following conditions: The function W consists of a logarithmic function, so it is clear that the function is a continuous function on P, and the first partial derivative is also a continuous function on P.

The function W has a global minimum at $\mathbb{E}^*$ with respect to all points in P.

For $W(S,E,I,Q) \neq W(S^0,E^0,I^0,Q^0)$ will be shown that $W(S,E,I,Q) > 0$.

$$W = \left(S - S^* - S^* ln\frac{S}{S^*}\right) + \left(E - E^* - E^* ln\frac{E}{E^*}\right) + \left(I - I^* - I^* ln\frac{I}{I^*}\right) + \left(Q - Q^* - Q^* ln\frac{Q}{Q^*}\right)$$

$= S^*\left(\frac{S}{S^*} - 1 - S^* ln\frac{S}{S^*}\right) + E^*\left(\frac{E}{E^*} - 1 - E^* ln\frac{E}{E^*}\right) + I^*\left(\frac{I}{I^*} - 1 - I^* ln\frac{I}{I^*}\right) + Q^*\left(\frac{Q}{Q^*} - 1 - Q^* ln\frac{Q}{Q^*}\right)$

It can be seen that the function W will be positive if $S^*\left(\frac{S}{S^*} - 1 - ln\frac{S}{S^*}\right) > 0, E^*\left(\frac{E}{E^*} - 1 - E^* ln\frac{E}{E^*}\right) > 0,\ I^*\left(\frac{I}{I^*} - 1 - I^* ln\frac{I}{I^*}\right) > 0\ and\ Q^*\left(\frac{Q}{Q^*} - 1 - Q^* ln\frac{Q}{Q^*}\right) > 0.$

The next step is to show the equilibrium point (S^*, E^*, I^*, Q^*) is the global minimum point which is done by obtaining the Hessian matrix in (S^*, E^*, I^*, Q^*):

$$H(S^*, E^*, I^*, Q^*) = \begin{bmatrix} \frac{\partial^2 W}{\partial S^2} & \frac{\partial^2 W}{\partial S \partial E} & \frac{\partial^2 W}{\partial S \partial I} & \frac{\partial^2 W}{\partial S \partial Q} \\ \frac{\partial^2 W}{\partial S \partial E} & \frac{\partial^2 W}{\partial E^2} & \frac{\partial^2 W}{\partial I \partial E} & \frac{\partial^2 W}{\partial Q \partial E} \\ \frac{\partial^2 W}{\partial S \partial I} & \frac{\partial^2 W}{\partial E \partial I} & \frac{\partial^2 W}{\partial I^2} & \frac{\partial^2 W}{\partial Q \partial I} \\ \frac{\partial^2 W}{\partial S \partial Q} & \frac{\partial^2 W}{\partial E \partial Q} & \frac{\partial^2 W}{\partial I \partial Q} & \frac{\partial^2 W}{\partial Q^2} \end{bmatrix} = \begin{bmatrix} 1/S^* & 0 & 0 & 0 \\ 0 & 1/E^* & 0 & 0 \\ 0 & 0 & 1/I^* & 0 \\ 0 & 0 & 0 & 1/Q^* \end{bmatrix}$$

Matrix $H(S^*, E^*, I^*, Q^*)$ positive definite because $\det\left(H(S^*, E^*, I^*, Q^*)\right) = \frac{1}{S^* E^* I^* Q^*} > 0$

For $W(S, E, I, Q) = W(S^*, E^*, I^*, Q^*)$ will be shown that $W(S, E, I, Q) = 0$.

$W = \left(S - S^* - S^* ln\frac{S}{S^*}\right) + \left(E - E^* - E^* ln\frac{E}{E^*}\right) + \left(I - I^* - I^* ln\frac{I}{I^*}\right) + \left(Q - Q^* - Q^* ln\frac{Q}{Q^*}\right)$

$= (0 - S^* ln1) + (0 - E^* ln1) + (0 - I^* ln1) + (0 - Q^* ln1)$

$= 0$

Then it is proved that $W(S, E, I, Q) > 0$ when $W(S, E, I, Q) \neq W(S^*, E^*, I^*, Q^*)$ with $W(S, E, I, Q) \in P$, dan $W(S, E, I, Q) = 0$ when $W(S, E, I, Q) = W(S^*, E^*, I^*, Q^*)$, as well as (S^*, E^*, I^*, Q^*) is the global minimum.

The derivative of the function W(t) is $\frac{dW(t)}{dt}$ satisfies $\frac{dW(t)}{dt} \leq 0$ for all points in P.

$\frac{dW}{dt} = \frac{\partial W}{\partial S}\frac{dS}{dt} + \frac{\partial W}{\partial E}\frac{dE}{dt} + \frac{\partial W}{\partial I}\frac{dI}{dt} + \frac{\partial W}{\partial Q}\frac{dQ}{dt}$

$= \left(1 - \frac{S^*}{S}\right)\frac{dS}{dt} + \left(1 - \frac{E^*}{E}\right)\frac{dE}{dt} + \left(1 - \frac{I^*}{I}\right)\frac{dI}{dt} + \left(1 - \frac{Q^*}{Q}\right)\frac{dQ}{dt}$

$= \left(1 - \frac{S^*}{S}\right)(\lambda - \beta SI - (\nu + \mu)S) + \left(1 - \frac{E^*}{E}\right)(\beta SI - (\alpha + \theta + \mu)E) + \left(1 - \frac{I}{I^*}\right)(\alpha E - (\gamma + \kappa + \mu)I) + \left(1 - \frac{Q^*}{Q}\right)(\theta E + \kappa I - (\gamma + \mu)Q)$

$= \left(1 - \frac{S^*}{S}\right)(\lambda - \beta SI - c_1 S) + \left(1 - \frac{E^*}{E}\right)(\beta SI - c_2 E) + \left(1 - \frac{I^*}{I}\right)(\alpha E - c_3 I) + \left(1 - \frac{Q^*}{Q}\right)(\theta E + \kappa I - c_4 Q)$

$$= \beta S^* I^* \left(2 - \frac{S^*}{S}\right) + c_1 S^* \left(2 - \frac{S^*}{S} - \frac{S}{S^*}\right) + \beta S^* I \left(1 - \frac{E^*}{E}\frac{S}{S^*}\right) + \alpha E^* \left(1 - \frac{I^*}{I}\frac{E}{E^*} + \frac{E}{E^*}\right) + \theta E^* \left(1 - \frac{Q^*}{Q} + \frac{E}{E^*} - \frac{E}{E^*}\frac{Q^*}{Q}\right) + \kappa I^* \left(1 - \frac{Q^*}{Q} + \frac{I}{I^*} - \frac{I}{I^*}\frac{Q^*}{Q}\right) + c_4 Q^* \left(1 - \frac{Q}{Q^*}\right) - c_2 E - c_3 I$$

$$= \left(2 - \frac{S^*}{S} - \frac{S}{S^*}\right)\left(\frac{(\Re_0 - 1)(\nu+\mu)(\alpha+\theta+\mu)(\gamma+\kappa+\mu)}{\beta(\alpha+\theta+\mu)(\gamma+\kappa+\mu)}\right)\beta S^* - c_1\left(\frac{S-S^*}{S}\right)^2 + (\theta E^* + \kappa I^*)\left(3 - \frac{2Q^*}{Q} - \frac{Q}{Q^*}\right)$$

According to the AM-GM Theorem we get $\frac{S^*}{S} + \frac{S}{S^*} \geq 2$ and $\frac{2Q^*}{Q} + \frac{Q}{Q^*} \geq 3$ that shown $\left(2 - \frac{S^*}{S} - \frac{S}{S^*}\right)$ and $\left(3 - \frac{2Q^*}{Q} - \frac{Q}{Q^*}\right)$ is the negative value. If the value of $\left(2 - \frac{S^*}{S} - \frac{S}{S^*}\right)$ and $\left(3 - \frac{2Q^*}{Q} - \frac{Q}{Q^*}\right)$ is negative and the value of $\Re_0 > 1$, then the value of $\frac{dW(t)}{dt} \leq 0$. Derivative of function W(t) is $\frac{dW(t)}{dt}$ fullfill of $\frac{dW(t)}{dt} \leq 0$ for all points in P, it can be concluded that the endemic equilibrium points E^* for the system of equations (1) is globally asymptotically stable.

Based on the discussion above, some key points regarding disease equilibria can be summarized:

- The disease-free equilibrium E^0, always exists regardless of parameter values.
- If the basic reproduction number, $\Re_0$, is less than 1, then only E^0 exists and it is globally asymptotically stable, meaning no endemic persists long-term.
- However, if $\Re_0$ exceeds 1, the endemic equilibrium, E^*, co-exists with E^0 and becomes globally asymptotically stable instead, such that the disease can persist long-term.
- As referenced in (Martcheva 2014) , this scenario typifies a forward bifurcation driven by the value of $\Re_0$
- Since $\Re_0$ is directly proportional to the infection rate β, variations in β can likewise induce the forward bifurcation.

Computational simulations were performed using the parameter values in **Table 1.** while modulating β. The resultant bifurcation diagram plotted in Figure 5 demonstrates the forward bifurcation, with the bifurcation point occurring when $\Re_0$ equals 1, equivalent to β approximately 0.00165.

Runge Kutta 5th Order Method

By following the steps for solving the Runge-Kutta method of order 5 equation (1) can be discretized into the following equation:

$$S_1 = S_0 + \frac{1}{90}\left(7k_{1,s} + 32k_{3,s} + 12k_{4,s} + 32k_{5,s} + 7k_{6,s}\right)h$$

$$E_1 = E_0 + \frac{1}{90}\left(7k_{1,E} + 32k_{3,E} + 12k_{4,E} + 32k_{5,E} + 7k_{6,E}\right)h$$

$$I_1 = I_0 + \frac{1}{90}\left(7k_{1,I} + 32k_{3,I} + 12k_{4,I} + 32k_{5,I} + 7k_{6,I}\right)h$$

$$Q_1 = Q_0 + \frac{1}{90}\left(7k_{1,Q} + 32k_{3,Q} + 12k_{4,Q} + 32k_{5,Q} + 7k_{6,Q}\right)h$$

$$R_1 = R_0 + \frac{1}{90}\left(7k_{1,R} + 32k_{3,R} + 12k_{4,R} + 32k_{5,R} + 7k_{6,R}\right)h$$

$$D_1 = D_0 + \frac{1}{90}\left(7k_{1,D} + 32k_{3,D} + 12k_{4,D} + 32k_{5,D} + 7k_{6,D}\right)h$$

Henceforth, the discretization results are used to complete numerical simulations with the help of the MATLAB software application.

Numerical Simulation

We verified our model and findings by using the Data of the Covid-19 spread in West Java Province from March 16, 2022 to April 16, 2022, obtained from https://pikobar.jabarprov.go.id/ and https://www.bps.go.id/, as well as data parameters obtained from calculations using the Least Square method with Maple tools and non-linear regression with MATLAB tools, so that the literature study is obtained in the following table.

Table 1. Parameter Value

Parameter	Initial Value	Unit	Source
λ	37.412	/Day	*[fitted]*
β	0.66501×10^{-6}	/Day	*[fitted]*
α	0.2	/Day	*[fitted]*
θ	0.409	/Day	*[fitted]*
κ	0.796	/Day	*[fitted]*
γ	0.274	/Day	*[fitted]*
ε_1	0.999	/Day	*[fitted]*
ε_2	0.135	/Day	*[fitted]*
μ	0.37×10^{-4}	/Day	*[fitted]*
ν	0.0189	/Day	*[fitted]*

Source: Prepared by the author (2024)

The initial values for our study (obtained from 16th of March data) are the following: $S(0) = 16{,}006{,}309, E(0) = 572{,}979, I(0) = 1{,}080{,}322, \mathrm{Q}(0) = 989{,}911, and\ D(0) = 15466$

The disease-free (non-endemic) equilibrium point is:

$$\mathbb{E}^0 = (S^0, E^0, I^0, Q^0) = \left(\frac{\lambda}{(\nu+\mu)}, 0,0,0\right) = (1975.603316; 0; 0; 0)$$

The calculation of the basic reproduction number ($\Re_0$) involves putting the parameter values from Table 1 into the following equation,

$$\Re_0 = \frac{\alpha\beta\lambda}{(\alpha+\theta+\mu)(\nu+\mu)(\gamma+\kappa+\mu)}$$

$$\Re_0 = 0.0004032$$

Based on this simulation, the value of $\Re_0 < 1$, so that in a long time the spread of the disease will decrease and in the end no individual will be infected with the Covid-19 virus.

Furthermore, using the calculation results obtained the eigenvalues of the Jacobian matrix at the non-endemic equilibrium point. By using Maple computational tools, the eigenvalues of the Jacobian matrix at the non-endemic equilibrium point are obtained as follows:

$$x_1 = -0.018937$$

$$x_2 = -0.274037$$

$$x_3 = -1.070606274$$

$$x_4 = -0.6084677263$$

Since the real part of all the eigenvalues is negative, the non-endemic equilibrium point is locally asymptotically stable. Next, we will analyse the global stability at the non-endemic equilibrium point using the Lyapunov function as follows.

$$\frac{dV(t)}{dt} = (\Re_0 - 1)(\alpha+\theta+\mu)E$$

$$\frac{dV(t)}{dt} = -0.6087914391$$

$\frac{dV(t)}{dt} < 0$ for $(S, E, I, Q, R, D) \in P$

Because the Lyapunov function can be found at the non-endemic equilibrium point, it can be concluded that the non-endemic equilibrium point is globally asymptotically stable.

Figure 2: Covid-19 Spread Simulation Graph

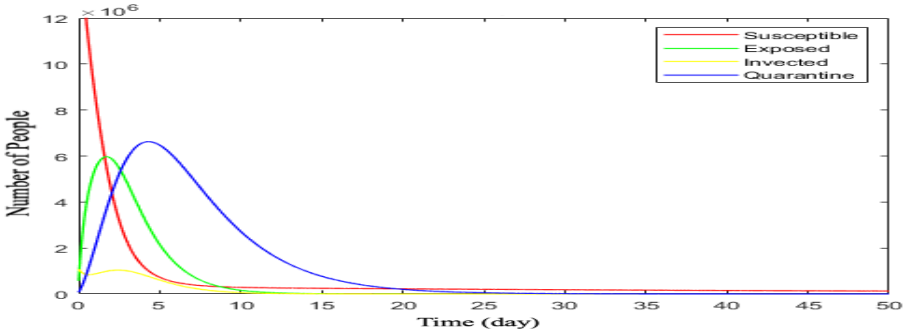

Figure 2 above shows the change in the number of SEIQ subpopulations over time in non-endemic cases. In the initial conditions, the number of Susceptible/vulnerable subpopulations decreased due to contact between susceptible individuals and infected individuals, so that susceptible individuals became latent individuals. In the Exposed/latent subpopulation, there was an increase, but then it decreased due to the change of latent individuals into infected individuals. In the Infected subpopulation, the spread of the virus increased in the initial state, then decreased due to the quarantine/isolation rate in the infected subpopulation. In the Quarantine/quarantine subpopulation, there was an increase at the beginning, but then it decreased due to changes in quarantine individuals to recover or die individuals.

Sensitivity Analysis

Sensitivity analysis is calculated by finding the partial derivative of $\mathfrak{R}_0$ with respect to the parameter (p).

$$C_p^{\mathfrak{R}_0} = \frac{\partial \mathfrak{R}_0}{\partial p} \times \frac{p}{\mathfrak{R}_0}$$

With the help of the Maple computational tool, we obtain the parameter sensitivity index in $\mathfrak{R}_0$ is as shown following table.

Table 2. Parameter Sensitivity Index

Parameter	Sensitivity Index
λ	1
β	1
α	0.6716127262
μ	-0.002049176856
γ	-0.2560659118
θ	-0.6716127262
κ	-0.7438995101
ν	-0.9980461530

Source: Prepared by the author (2024)

Based on the sensitivity index values provided in Table 2:

- The four parameters with the most significant impacts on COVID-19 spread, in descending order of effect, are: recruitment rate (λ), transmission rate from Susceptible to Infected (β), incubation period transition rate (α), and the natural mortality rate (μ).
- λ, β, and μ each carry positive sensitivity indices. Therefore, increasing these parameter values serves to elevate the basic reproduction number R0, augmenting viral dissemination.
- Conversely, $\mu, \gamma, \theta, \kappa$, and ν exhibit negative sensitivity indices. A rise in any of these parameters acts to decrease $\Re_0$, curbing pandemic propagation.
- Specifically, higher recovery (γ) and isolation (θ, κ) rates, together with increased vaccination (ν), help limit transmission opportunities by shortening infection durations and removing infectious sources.

In summary, the recruitment rate, transmission probability, and incubation onset pace promote the pandemic according to this analysis, while faster recovery, more proactive isolation, and expanded immunization dampen contagiousness as quantified by their negative impacts on $\Re_0$.

To further elucidate how influential parameters affect disease progression, simulations were conducted examining variations in those parameters demonstrating high sensitivity, namely $\alpha, \mu, and\ \nu$:

Figure 3 depicts the impact on infected numbers (I) when only α, the incubation period transition rate, is altered while other values remain fixed. Specifically, simulations were run with $\alpha = 0.079, 0.416, and\ 0.985$. The results clearly show that higher α values, corresponding to faster development of symptoms after exposure, produce significantly fewer total infected individuals over time. With $\alpha = 0.079$, I reaches 12915 by day 14, compared to only 978 for $\alpha = 0.416$ and 42 $for\ \alpha = 0.985$.

Figure 3: The impact of varying the value of α on the infected population

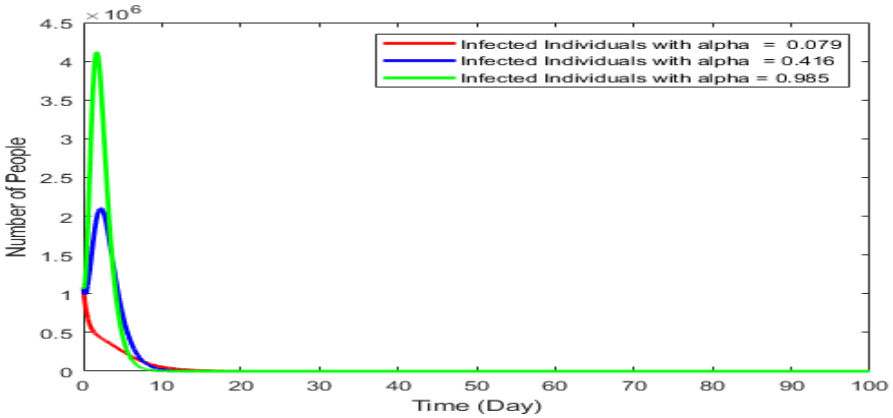

This corroborates the positive sensitivity of α, confirming faster symptom onset helps curb pandemic expansion by reducing the duration infectious subjects can potentially transmit the virus while asymptomatic. Control strategies aimed at shortening incubation periods may thus prove beneficial from an epidemiological modelling perspective according to these explorations.

Figure 4 depicts the impact on the number of infected individuals (I) when only the natural mortality rate (μ) is varied between 0.079, 0.416, and 0.985 while holding other parameters constant.

It can be clearly seen that higher μ values, corresponding to increased baseline mortality, produce markedly fewer total infections over the 14-day period. Specifically:

- With $\mu = 0.079$, I reaches a peak of 2426 individuals by day 14.
- For $\mu = 0.416$, the maximum I is reduced to only 9 cases.
- And with $\mu = 0.985$, no infected cases emerge, as any new infections are immediately offset by the very high background death rate.

Figure 4: The impact of varying the value of μ on the infected population

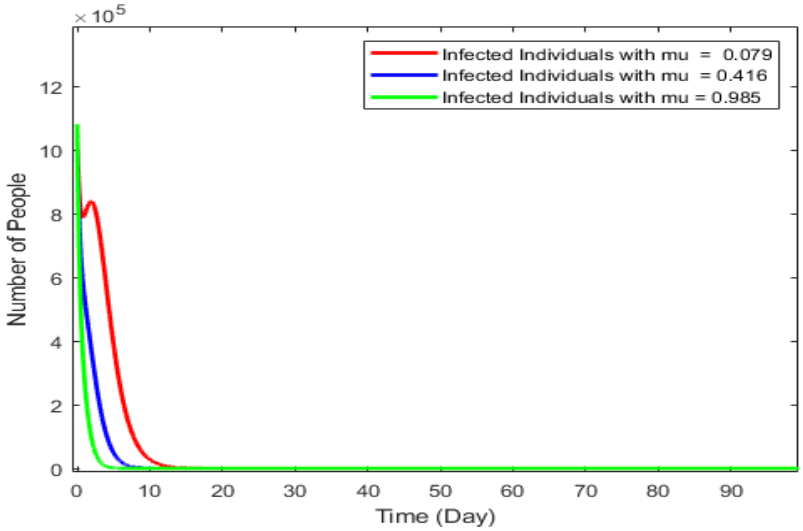

Therefore, in accordance with the negative sensitivity of μ identified earlier, elevating the natural removal of individuals from the population through death helps effectively curb pandemic spread over time by limiting opportunities for disease transmission. Strategies to maintain overall public health standards may complement other interventions from this perspective.

Figure 5 illustrates the impact on the number of infected individuals (I) when only the vaccination rate of susceptible persons (ν) is altered between 0.079, 0.416, and 0.985 while holding other factors fixed. Notably, increasing ν yields progressively fewer total infections over the 14-day span depicted. Specifically:

- With $\nu = 0.079$, the peak I reaches 5068 cases.
- At $\nu = 0.416$, the maximum I declines substantially to 1801 cases.
- And for $\nu = 0.985$, an even sharper reduction occurs, capping I at approximately 790 cases.

Figure 5: The impact of varying the value of ν on the infected population

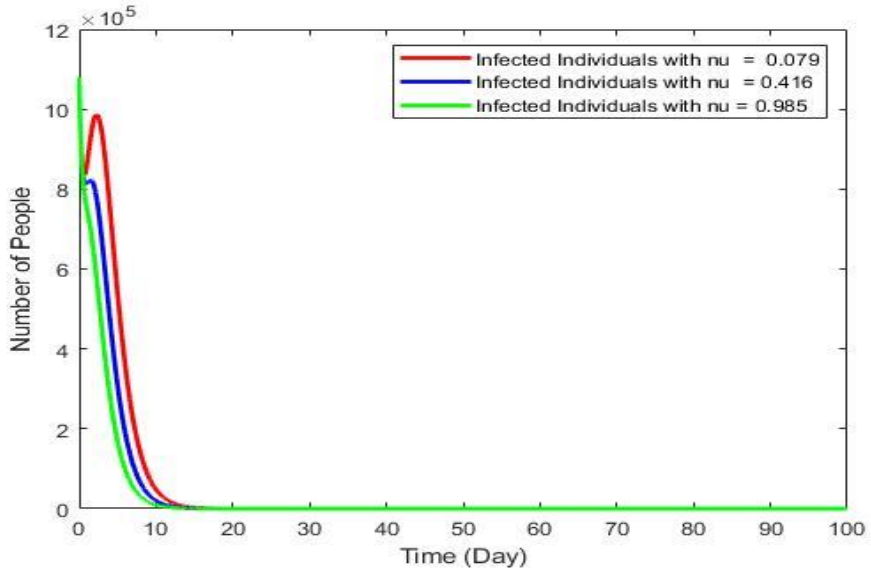

Consistent with the protective influence of higher vaccination proposed by the negative sensitivity of ν, these simulations confirm expanded immunization programs help suppress pandemic growth over time by lowering the availability of susceptible hosts. More robust vaccine rollout aligns well with curbing communal spread according to this investigative modelling work.

Figure 6: Forward bifurcation driven by $\mathfrak{R}_0$

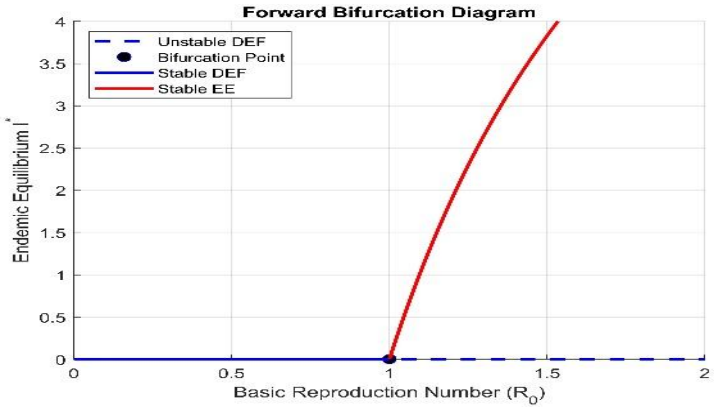

Figure 6. shows that the system (1) experiences a forward bifurcation at $\mathfrak{R}_0 = 1$ corresponding to the infection rate value of $\beta \cong 0.00165$. by observing Figure 6. We can notice that the disease-free equilibrium which is feasible always loses its stability when $\mathfrak{R}_0 > 1$ while the endemic equilibrium becomes feasible and stable at the same period of $\mathfrak{R}_0 > 1$.

Conclusion

This study developed a SEIQRD compartmental model to simulate the spread of COVID-19 among six interacting subgroups: susceptible (S), exposed/latent (E), infected/symptomatic (I), quarantined (Q), recovered/immune (R), and deaths (D).Local stability of the disease-free and endemic equilibria was evaluated using the Routh-Hurwitz criteria. This analytical approach provided results for the local asymptotic stability at both non-endemic and endemic states. Global stability was also investigated via the Lyapunov method. This numerical technique similarly yielded conclusions about the global asymptotic stability at the non-endemic and endemic equilibria.

By dividing the population into these six subclasses and applying mathematical modelling frameworks like Routh-Hurwitz and Lyapunov analyses, the research afforded a more nuanced understanding of disease dynamics compared to simpler formulations. The stability determinations at equilibrium conditions offer useful prognostic insights into how perturbations may influence long-term propagation under different transmission scenarios. The key findings from the mathematical modelling and analysis were. Numerical simulations computed a basic reproduction number ($\mathfrak{R}_0$ less than 1. With $\mathfrak{R}_0 < 1$, the disease-free equilibrium is locally and globally asymptotically stable according to the analytical techniques applied. Therefore, in the long run the spread of COVID-19 through the population will decrease such that eventually no individuals remain infected. Sensitivity analysis identified four parameters with primary influence on transmission dynamics. Recruitment rate into the susceptible class Transmission probability from susceptible to infected individuals Onset rate from latent to symptomatic phase

Natural mortality rate Of these, faster progression to symptoms post-exposure, higher baseline removal of individuals from the population, and increased vaccination reduced infected over time Conversely, higher recruitment feeding the susceptible reservoir and enhanced transmission boosted pandemic progression In conclusion, the modelling elucidated which epidemiological factors most significantly drive the reproduction number and should therefore guide mitigation response prioritization.

Acknowledgments

This work is supported by Diponegoro University, Indonesia, under RPI Research Grant with contract number 233-26/UN7.6.1/PP/2020-2021. This research was supported by the Laboratory of Computer Modelling, Mathematics Department, Faculty of Science and Mathematics, Diponegoro University, Semarang, Indonesia

References

Levani, Y., Prastya, A. D., & Mawaddatunnadila, S. (2021). Coronavirus Disease 2019 (COVID-19): Patogenesis, Manifestasi Klinis dan Pilihan Terapi. *Jurnal Kedokteran Dan Kesehatan*, *17*(1), 44. https://doi.org/10.24853/jkk.17.1.44-57

Mukherjee, A., Pandey, K. M., Ojha, K. K., & Sahu, S. K. (2023). Identification of possible SARS-CoV-2 main protease inhibitors: in silico molecular docking and dynamic simulation studies. *Beni-Suef University Journal of Basic and Applied Sciences*, *12*(1). https://doi.org/10.1186/s43088-023-00406-4

Peter, O. J., Qureshi, S., Yusuf, A., Al-Shomrani, M. M., & Abioye, A. I. (2021). A new mathematical model of COVID-19 using real data from Pakistan. *Results in Physics*, *24*, 104098. https://doi.org/10.1016/j.rinp.2021.104098

Khan, J., Asoom, L. I. A., Khan, M., Chakrabartty, I., Dandoti, S., Rudrapal, M., & Zothantluanga, J. H. (2021). Evolution of RNA viruses from SARS to SARS-CoV-2 and diagnostic techniques for COVID-19: a review. *Beni-Suef University Journal of Basic and Applied Sciences*, *10*(1). https://doi.org/10.1186/s43088-021-00150-7

Sherif, B., Hafez, H., Abdelhalim, M. R., Elwafa, M. a. Z. A., Wahba, N. S., & Hamdy, P. (2023). Evaluation of diagnostic performance of SARS-CoV-2 detection kits: a comparative study. *Beni-Suef University Journal of Basic and Applied Sciences*, *12*(1). https://doi.org/10.1186/s43088-023-00360-1

Legesse, F. M., Rao, K. P., & Keno, T. D. (2023). Mathematical Modeling of a Bimodal Pneumonia Epidemic with Non-breastfeeding Class. *Applied Mathematics & Information Sciences*, *17*(1), 95–107. https://doi.org/10.18576/amis/170111

Nasution, N. H., & Hidayah, A. (2021). Gambaran Pengetahuan Masyarakat Tentang Pencegahan Covid-19 Di Kecamatan Padangsidimpuan Batunadua, Kota Padangsidimpuan. *Jurnal Kesehatan Ilmiah Indonesia (Indonesian Health Scientific Journal)*, *6*(1), 107. https://doi.org/10.51933/health.v6i1.419

Han, Y., & Yang, H. (2020). The transmission and diagnosis of 2019 novel coronavirus infection disease (COVID-19): A Chinese perspective. *Journal of Medical Virology*, *92*(6), 639–644. https://doi.org/10.1002/jmv.25749

Wu, F., Zhao, S., Yu, B., Chen, Y. M., Wang, W., Song, Z., Hu, Y., Zhao, T., Tian, J., Yuan, P., Yuan, M., Zhang, Y. L., Dai, F. H., Liu, Y., Wang, Q. M., Zheng, J., Xu, L., Holmes, E. C., & Zhāng, Y. Z. (2020). A new coronavirus associated with human respiratory disease in China. *Nature*, *579*(7798), 265–269. https://doi.org/10.1038/s41586-020-2008-3

Letko, M., Marzi, A., & Munster, V. J. (2020). Functional assessment of cell entry and receptor usage for SARS-CoV-2 and other lineage B betacoronaviruses. *Nature Microbiology*, *5*(4), 562–569. https://doi.org/10.1038/s41564-020-0688-y

Sinaga, L. P., Nasution, H. I., & Kartika, D. (2021). Stability Analysis of the Corona Virus (COVID-19) Dynamics SEIR model in Indonesia. *Journal of Physics: Conference Series*, *1819*(1), 012043. https://doi.org/10.1088/1742-6596/1819/1/012043

Fatima, B. B., Zaman, G., Alqudah, M. A., & Abdeljawad, T. (2021). Modeling the pandemic trend of 2019 Coronavirus with optimal control analysis. *Results in Physics*, *20*, 103660. https://doi.org/10.1016/j.rinp.2020.103660

Yang, C., & Wang, J. (2020). A mathematical model for the novel coronavirus epidemic in Wuhan, China. *Mathematical Biosciences and Engineering*, *17*(3), 2708–2724. https://doi.org/10.3934/mbe.2020148

Schecter, S. (2021). Geometric singular perturbation theory analysis of an epidemic model with spontaneous human behavioral change. *Journal of Mathematical Biology*, *82*(6). https://doi.org/10.1007/s00285-021-01605-2

Kolawole, M. K., Olayiwola, M. O., Alaje, A. I., Adekunle, H. O., & Odeyemi, K. A. (2023). Conceptual analysis of the combined effects of vaccination, therapeutic actions, and human subjection to physical constraint in reducing the prevalence of COVID-19 using the homotopy perturbation method. *Beni-Suef University Journal of Basic and Applied Sciences*, *12*(1). https://doi.org/10.1186/s43088-023-00343-2

Sahu, L. K., & Singh, R. (2023). Cross-variant proof predictive vaccine design based on SARS-CoV-2 spike protein using immunoinformatics approach. *Beni-Suef University Journal of Basic and Applied Sciences*, *12*(1). https://doi.org/10.1186/s43088-023-00341-4

Savina, K. F., Sreekumar, R., Soonu, V. K., & Variyar, E. J. (2022). Various vaccine platforms in the field of COVID-19. *Beni-Suef University Journal of Basic and Applied Sciences*, *11*(1). https://doi.org/10.1186/s43088-022-00215-1

Shah, N. H., & Mittal, M. (2021). *Mathematical Analysis for Transmission of COVID-19*. Springer Nature.

Hamed, A. M. (2022). Modeling of corona virus and its application in confocal microscopy. *Beni-Suef University Journal of Basic and Applied Sciences*, *11*(1). https://doi.org/10.1186/s43088-022-00276-2

Shah, N. H., & Chaudhary, K. (2023). Analysis of the Ebola with a fractional-order model involving the Caputo-Fabrizio derivative. *Songklanakarin Journal of Science & Technology*, *45*(1), 69.

Hossain, M. B. (2017). A Comparative Study on Fourth Order and Butcher's Fifth Order Runge-Kutta Methods with Third Order Initial Value Problem (IVP). *Applied and Computational Mathematics*, *6*(6), 243. https://doi.org/10.11648/j.acm.20170606.12

Owolabi, K. M., & Atangana, A. (2019). Mathematical analysis and computational experiments for an epidemic system with nonlocal and nonsingular derivative. *Chaos, Solitons & Fractals*, *126*, 41–49. https://doi.org/10.1016/j.chaos.2019.06.001

Parsamanesh, M., Erfanian, M., & Mehrshad, S. (2020). Stability and bifurcations in a discrete-time epidemic model with vaccination and vital dynamics. *BMC Bioinformatics*, *21*(1). https://doi.org/10.1186/s12859-020-03839-1

Annas, S., Pratama, M. I., Rifandi, M., Sanusi, W., & Side, S. (2020). Stability analysis and numerical simulation of SEIR model for pandemic COVID-19 spread in Indonesia. *Chaos, Solitons & Fractals*, *139*, 110072. https://doi.org/10.1016/j.chaos.2020.110072

Kamrujjaman, M., Saha, P., Islam, M. S., & Ghosh, U. (2022). Dynamics of SEIR model: A case study of COVID-19 in Italy. *Results in Control and Optimization*, *7*, 100119. https://doi.org/10.1016/j.rico.2022.100119

Chapra, S. C., & Canale, R. P. (2015). *Numerical Methods for Engineers*. McGraw-Hill Education.

Mamo, D. K. (2020). Model the transmission dynamics of COVID-19 propagation with public health intervention. *Results in Applied Mathematics*, *7*, 100123. https://doi.org/10.1016/j.rinam.2020.100123

Saeed, R. M. (2017). Achieve asymptotic stability using Lyapunov's second method. *IOSR Journal of Mathematics*, *13*(01), 72–77. https://doi.org/10.9790/5728-1301017277

Gaber, T., Herdiana, R., & Widowati. (2024). Dynamical analysis of an eco-epidemiological model experiencing the crowding effect of infected prey. *Communications in Mathematical Biology and Neuroscience*. https://doi.org/10.28919/cmbn/8353

Martcheva, M. (2014). *An Introduction to Mathematical Epidemiology*. Springer.

Wintachai, P., & Prathom, K. (2021). Stability analysis of SEIR model related to efficiency of vaccines for COVID-19 situation. *Heliyon*, *7*(4), e06812. https://doi.org/10.1016/j.heliyon.2021.e06812

Nugroho, A. A. (2021). *Pemodelan matematis penyebaran virus sars-cov2 dan penyelesaian numerisnya menggunakan metode Runge-Kutta Orde Empat* [Skripsi]. Sanata Dharma University.

Mishra, A. M., Purohıt, S. D., Owolabi, K. M., & Sharma, Y. D. (2020). A nonlinear epidemiological model considering asymptotic and quarantine classes for SARS CoV-2 virus. *Chaos, Solitons & Fractals*, *138*, 109953. https://doi.org/10.1016/j.chaos.2020.109953